

## Preparation and Characterization of Precipitated Nano Hydroxyapatite

<sup>1</sup>Angelin Jeba Kala B and <sup>2</sup>Asaithambi T

<sup>1</sup>Department of Physics, Ponjesly College of Engineering, Kanyakumari District, Tamilnadu, India

<sup>2</sup>P.G & Research Department of Physics, Alagappa Government. Arts College, Karaikudi, Tamilnadu, India

**Correspondence Author:** Angelin Jeba Kala B, Department of Physics, Ponjesly College of Engineering, Kanyakumari District, Tamilnadu, India.  
E-mail: angelseath@gmail.com

**Received date:** 10 January 2018, **Accepted date:** 05 February 2018, **Online date:** 10 March 2018

**Copyright:** © 2018 Angelin Jeba Kala B. This is an open-access article distributed under the terms of the Creative Commons Attribution License, which permits unrestricted use, distribution, and reproduction in any medium, provided the original author and source are credited.

### Abstract

Calcium Hydroxyapatite [Ca<sub>10</sub>(PO<sub>4</sub>)<sub>6</sub>(OH)<sub>2</sub>] is the main inorganic constituent of human rigid tissues. It constitutes the major component of bone and enamel. In our present work, hydroxyapatite was synthesized by chemical co-precipitation method with the addition of different concentrations of calcium nitrate tetra hydrate [Ca(NO<sub>3</sub>)<sub>2</sub>.4H<sub>2</sub>O] and phosphoric acid [H<sub>3</sub>PO<sub>4</sub>] using micro wave irradiation. Experiments were conducted under controlled environment maintaining required pH, concentration of solution and temperature. The Present report emphasises on the synthesis and characterization of the nano hydroxyapatite. The result of Fourier Transform Infrared Spectroscopy [FTIR] showed the existence of the functional group present in hydroxyapatite. Scanning Electron Microscope [SEM] explains the surface morphology, size and dimensions of hydroxyl apatite. Thermo Gravimetric Analysis and Differential Thermal Analysis [TGA/DTA] analysis confirms that the high thermal stability of hydroxyapatite is due to the variation in concentration and its hardness is maximum.

**Key words:** Nano hydroxy apatite, Precipitation, FTIR, SEM, TGA/DTA

### INTRODUCTION

Calcium hydroxyapatite closely resembles human tooth and bone mineral and they are particularly attractive materials for their implants. It is the widely accepted biomaterial for the repair and reconstruction of bone tissue imperfection. Seventy percent of bone is made up of the mineral hydroxyapatite. In natural bone, the crystal size of hydroxyapatite is in nano range. The fundamental elements of hydroxyapatite are primarily calcium and Phosphorus with the stoichiometric ratio of 1.667. It has the characteristic features of biomaterials, such as biocompatible, bio-active, osteo conductive, non-toxic, non-inflammatory and non-immunogenic properties (Laura, 2015; John Michel, 2015; Sasikumar, 2006; Singh, 2012; Agrawal, 2011), it has been widely used in biomedical application such as tissue engineering system (Lv *et al.*, 2009), replacement for bony and periodontal defects (Trombelli *et al.*, 2010), bioactive coating on metallic osseous implants (Blackwood and Seah, 2009) and dental materials (Liu *et al.*, 2014).

Many clinical studies have successfully proved that hydroxyapatite shows good performance in terms of osseous ingrowth (Makela, 2008; Hayakawa, 2002; Darimont, 2002). Nano sized hydroxyapatite has a high surface activity and an ultra-fine structure. Similar to the mineral found in hard tissues (Vallet-Regi and Gonzalez-Calbet, 2004), it has been the most useful processing material for a variety of biomedical applications (Huang, 2007; Wu, 2015). In addition, nanosized hydroxyapatite shows improved densification and sinterability due to its high surface energy (Eriksson, 2011; Bianco, 2009). It promotes faster bone regeneration and direct bonding to the regenerated bone without intermediate connective tissue. Many research groups have developed preparative procedures for hydroxyapatite. It can be synthesized by reaction in solid state (Arita *et al.*, 1995), co-precipitation method (Akao, 1981; Kong, 2002), hydrothermal method (Zhang and Vecchio, 2007), sol-gel process (Wang and Shaw, 2009) and microwave processing (Yang *et al.*, 2002) method. In the present study, preparation and characterization of precipitated nanosized hydroxyapatite were carried out using the method of chemical co-precipitation. Hydroxyapatite are incurred from the reaction of inorganic chemical solution.

The objective of this present work is to obtain ultrafine hydroxyapatite particles which can be synthesized by chemical co-precipitation method in a technique of short processing time with a rapid heating method using different concentration of calcium nitrate tetra hydrate [Ca (NO<sub>3</sub>)<sub>2</sub>.4H<sub>2</sub>O] and phosphoric acid [H<sub>3</sub>PO<sub>4</sub>]. The thermally treated powder was characterized by FTIR, TGA/DTA and EDAX in order to identify the phase composition, functionality and thermal stability.

### MATERIALS AND METHODS

The starting materials used in the process were calcium nitrate tetra hydrate [Ca(NO<sub>3</sub>)<sub>2</sub>.4H<sub>2</sub>O] and phosphoric acid [H<sub>3</sub>PO<sub>4</sub>]. Ammonium hydroxide is used as pH regulating agent. Magnetic stirrer with heating facility for reaction mixture, pH metre, thermometer and weighing equipment were used.

#### 1.2.1 Synthesis of nano hydroxyapatite:

Chemical co-precipitation involves the use of aqueous solution, which leads to obtaining hydroxyapatite with high precise super facial area and small particle size distribution. In most of the cases, there will be difference in stoichiometry, at the same time the amorphous nature is obtained (Varma, 2005; Claudia, 2015; Ciobanu, 2015; Sooksanen, 2015; Galindo, 2015). It depends upon a number of influences such as reactants involved in synthesis, concentration and preliminary pH of solutions, reaction temperature etc., (Sasikumar and Vijayaraghavan, 2006). The final product of hydroxyapatite synthesized by the method of chemical co-precipitation results in high purity and crystalline, which is further characterized depends on a number of process, parameters such as synthesis temperature,

starting concentration of reactants involved in synthesis reaction, the pH of the reaction, the rate of acid addition, the stirring speed of the chemical substance and the condition of thermal treatment applied to as dried hydroxyapatite powders.

Nano hydroxyapatite was synthesized by chemical co-precipitation method. Ca/P ratio is maintained in the stoichiometry during the experiment and the basic is maintained to compare the result obtained. Aqueous solution of 0.5M calcium nitrate tetra hydrate  $[\text{Ca}(\text{NO}_3)_2 \cdot 4\text{H}_2\text{O}]$  and 0.5M phosphoric acid  $[\text{H}_3\text{PO}_4]$  were prepared.  $\text{H}_3\text{PO}_4$  was added drop by drop with the Ca/P ratio of 1:67 to the calcium nitrate tetra hydrate solution and was stirred for 30 minutes. After 30 minutes of mixing, ammonium hydroxide was mixed into the solution to form precipitate. It is constantly stirred for 30 minutes. pH value is determined using pH meter. The resultant was filtered. The hydroxyapatite powder obtained is washed repeatedly to remove the unwanted ions  $[\text{NH}_4^+$  and  $\text{NO}_3^-]$  and then set for drying at  $75^\circ\text{C}$  for 3 hours using an electric oven.

## RESULT AND DISCUSSION

### 1.3.1 Thermal Analysis:

TGA is used to understand the thermal properties of the sample. The thermal behaviour of hydroxyapatite was studied in the temperature range  $50^\circ\text{C} - 830^\circ\text{C}$  at a heating rate of  $10^\circ\text{C}/\text{min}$ . It was observed from the TGA curve that the first stage of weight loss occurred is due to the liberation of co-ordinated (bonded) water molecules. As the water molecules are liberated the sample becomes anhydrous (Sekar *et al.*, 2009). Decomposition started just above the room temperature and finally at  $817.6^\circ\text{C}$  it losses the weight of 11.33 %. The loss in weight may be due to the dehydration of water and ammonia in this temperature range.

In DTA analysis two sharp endothermic peaks are observed at  $76.64^\circ\text{C}$  and  $262.58^\circ\text{C}$ . The peak at  $76.64^\circ\text{C}$  is assigned to the decomposition point due to the release of water along with ammonium nitrate. Since the curve is almost constant it is inferred that there is no major loss in the sample which confirms the thermal stability. The following figure 1 shows TGA pattern of Nano Hydroxyapatite.

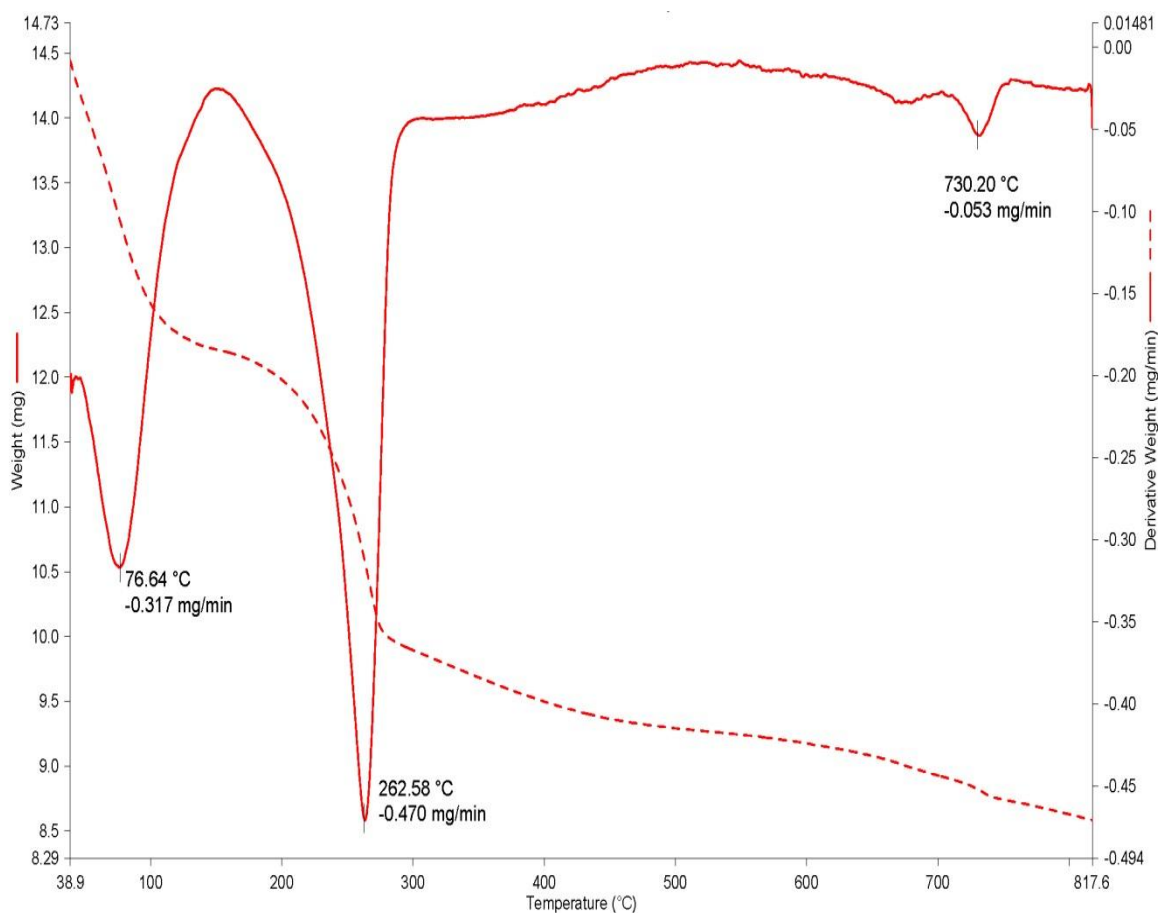
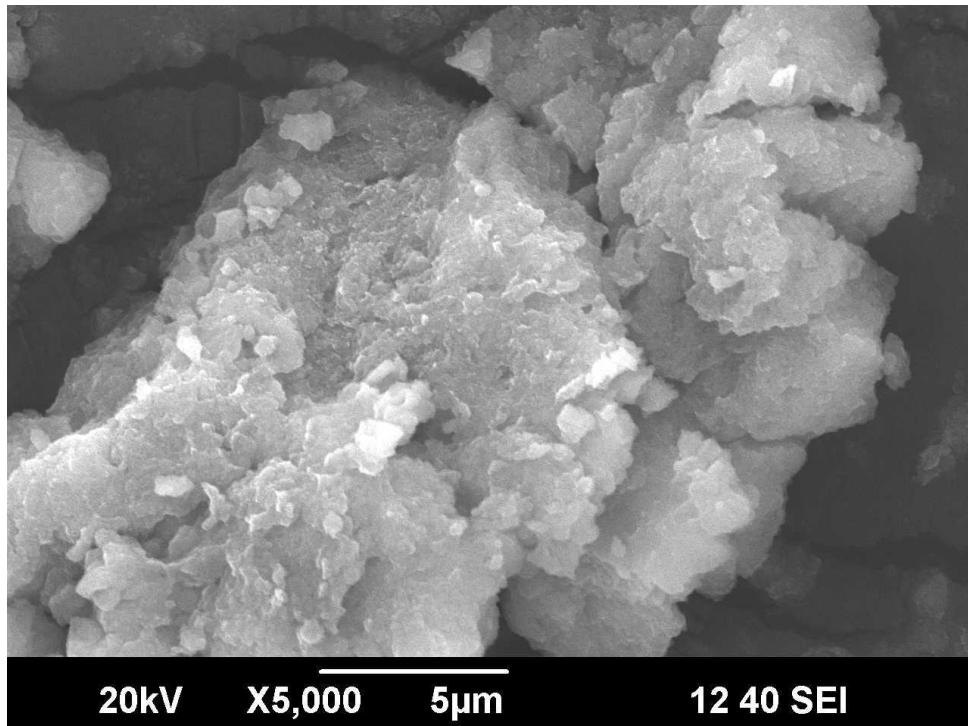


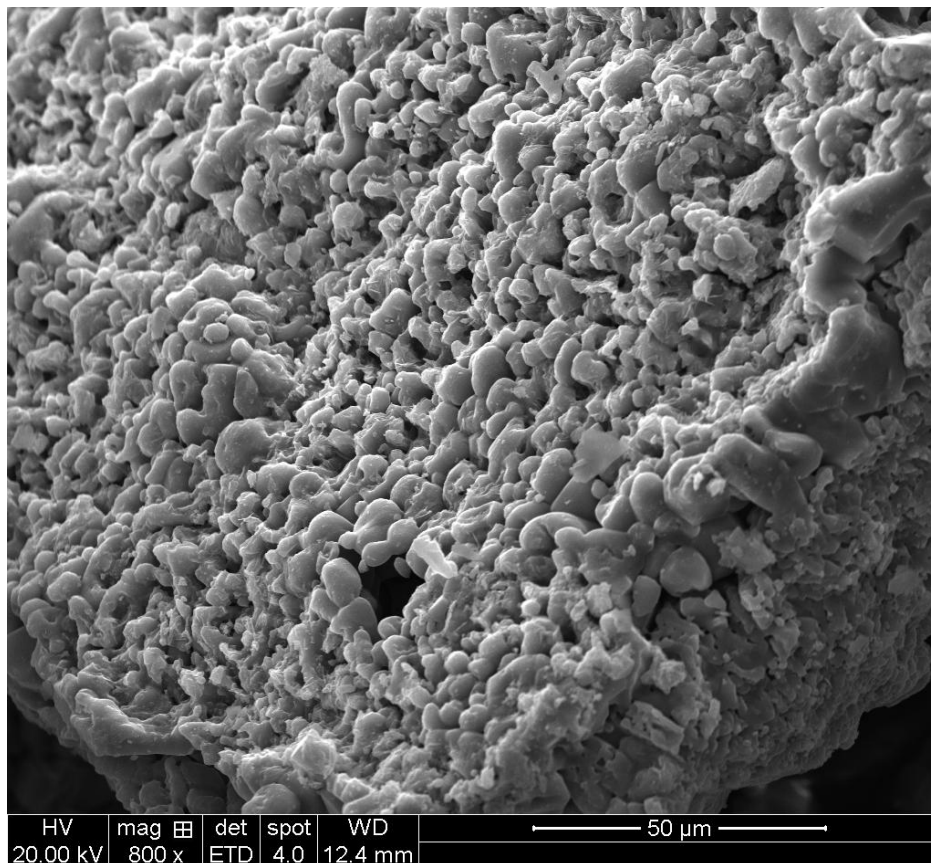
Fig. 1: TGA pattern of Nano Hydroxyapatite

### 1.3.2 SEM Analysis of hydroxyapatite:

SEM was used for the morphological study of nanoparticles of hydroxyapatite. The micro structure of SEM at normal temperature and  $300^\circ\text{C}$  is shown in figure 2. The synthesized hydroxyapatite is porous in nature. The presence of uniformly disseminated macroporous and microporous with in the pore walls can be seen in figure 2. The size and interconnectivity of pores determine the ability of the nutrient diffusion. Porosity and pore average size decreases with increase of mineral content and slightly increases in thickness. At normal temperature closed pores are formed. It can have a positive impact when used into the implant as it facilitates interaction between the implant and the biological environment (Claudia *et al.*, 2015). The following figure 2 shows SEM image of Nano Hydroxyapatite for Normal Temperature (a) and  $300^\circ\text{C}$  (b).



(a)



(b)

**Fig. 2:** SEM image of Nano Hydroxyapatite for Normal Temperature(a) and 300°C(b)

### 1.3.3 FTIR Analysis:

Infrared Spectroscopy is a way of doing chemical analysis by obtaining a spectrum. It has peaks and dips which suggests corresponding part of the spectrum being absorbed by the sample. The corresponding absorbed wave number is then matched with IR spectroscopy database to know the kind of functional group due to which the peak or dip has appeared. FTIR spectra of the prepared hydroxyapatite for 0.5M concentration of  $[\text{Ca}(\text{NO}_3)_2 \cdot 4\text{H}_2\text{O}]$  with 0.5M of  $[\text{H}_3\text{PO}_4]$  for (a) Normal temperature (b) 300°C (c) 600°C, was obtained. The following figure 3 shows FTIR spectra of Hydroxyapatite in (a) Normal Temperature (b) 300°C and (c) 600°C.

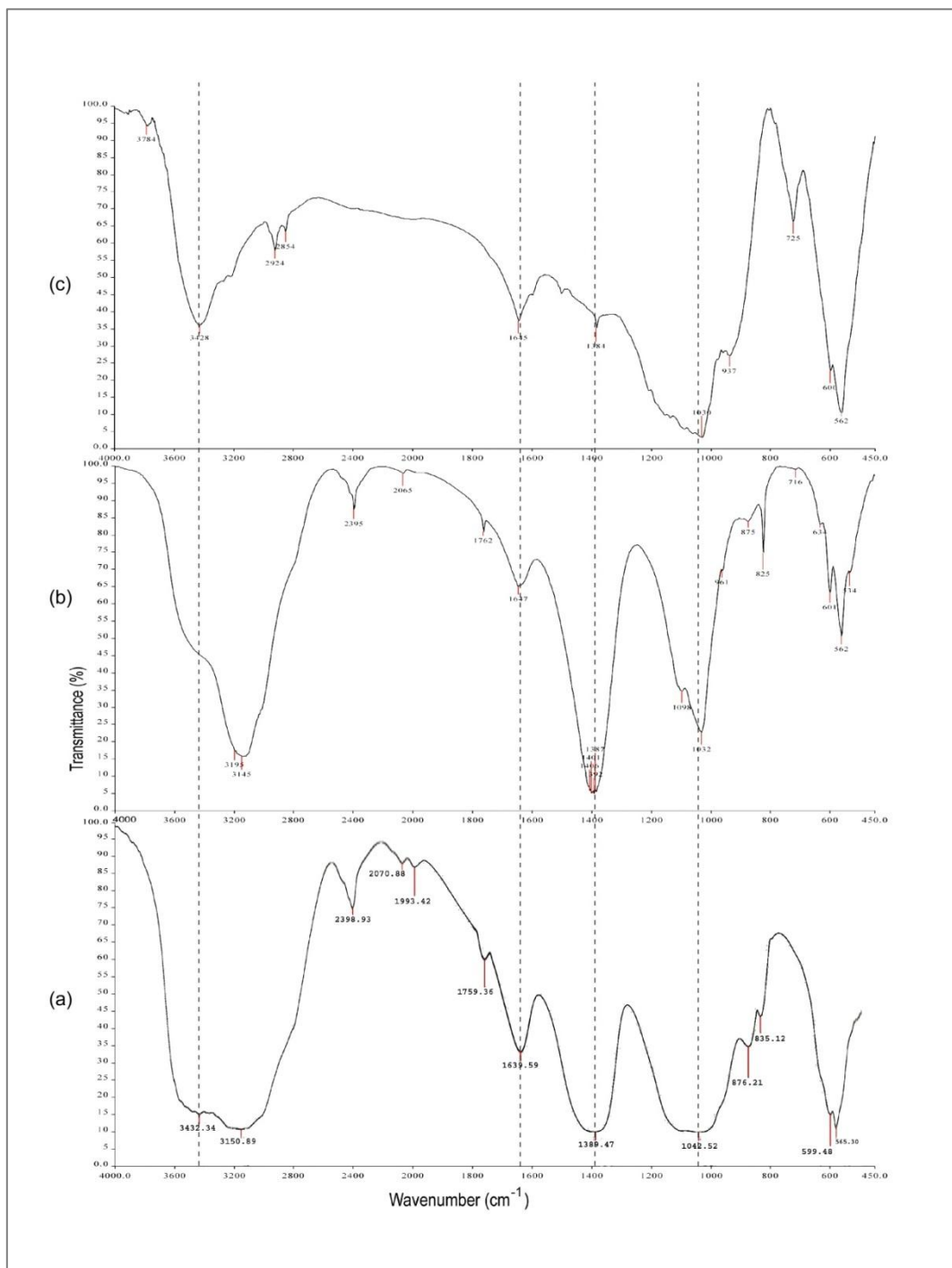


**Fig. 3:** FTIR spectra of Hydroxyapatite in (a) Normal Temperature (b) 300°C and (c) 600°C

From the obtained spectra, the sharp band at  $3432\text{cm}^{-1}$ ,  $3428\text{cm}^{-1}$  and  $3195\text{cm}^{-1}$  represents the stretching vibration of combined water in HA lattice (Meejoo *et al.*, 2006). As the heating temperature increases, the broad band in the region  $3150\text{cm}^{-1}$  would gradually narrow down. The liberational and stretching band of  $\text{OH}^-$  ions at  $634\text{cm}^{-1}$  and  $3784\text{cm}^{-1}$  gradually decreases in there intensity. When the temperature is over  $1300^\circ\text{C}$ , the liberated  $\text{OH}^-$  band disappears. The stretching band of  $\text{OH}^-$  ions was still absorbed for the wavenumbers  $1389\text{cm}^{-1}$ ,  $1384\text{cm}^{-1}$  and  $1387\text{cm}^{-1}$ . The absorption bands at  $1639\text{cm}^{-1}$ ,  $1645\text{cm}^{-1}$  and  $1647\text{cm}^{-1}$  was attributed to hydrogen phosphate  $\text{HPO}_4^{2-}$ . The bands centred at  $1042\text{cm}^{-1}$ ,  $1032\text{cm}^{-1}$  and  $1030\text{cm}^{-1}$  are obtained due to the symmetric and anti-symmetric stretching vibrations of the P-O bonds which are presented in  $\text{PO}_4^{3-}$ . Bands  $564.0\text{cm}^{-1}$ ,  $565.30\text{cm}^{-1}$  and  $562\text{cm}^{-1}$  shows the presence of  $\text{PO}_4^{3-}$  ions. The broad band at  $3150\text{cm}^{-1}$  and  $1759\text{cm}^{-1}$  where attributed to observed water. At higher temperature,  $\text{OH}^-$  stretching band seems more stabilized than the  $\text{OH}^-$  liberational mode. Even at a temperature upto  $1350^\circ\text{C}$ , the  $\text{OH}^-$  stretching band could be detected in the FTIR spectra. The large separation of the bands shows the presence of crystalline phase. Therefore it is obvious that the synthesised powder is certainly hydroxyapatite.

#### Conclusion:

Calcium hydroxyapatite was successfully synthesised using the easily available materials. From the FTIR analysis, the presence of the functional groups O-H,  $\text{HPO}_4^{2-}$  and  $\text{PO}_4^{3-}$  are confirmed. The intensity decreases with increase in temperature. Through SEM analysis it was found that the particles are in porous in nature. TGA/DTA analysis confirms that the loss due to dehydration. Minimum loss percentage is due to high thermal stability and it confirms the hardness of the synthesised hydroxyapatite. The future scope of this work would be rigorously carry out for various biocompatibility tests for clinical applications.

## REFERENCES

- Agrawal, K., S. Gurbhinder, P. Devendra, *et al.*, 2011. Synthesis and characterization of hydroxyapatite powder by sol-gel method for biomedical application. *Journal of Minerals and Materials Characterization and Engineering*, 10: 727-34.
- Akao M., H. Aoki and K. Kato, 1981. Mechanical properties of sintered hydroxyapatite for prosthetic applications. *Journal of Materials science*, 16(3): 809-812.
- Arita, I.H., V.M. Castano and D.S. Wilkinson, 1995. Synthesis and processing of hydroxyapatite ceramic tapes with controlled porosity, *Journal of Material Science: Material in Medicine*, 6(1): 19-23.
- Bianco, A., I. Cacciotti, M. Lombardi and L. Montanaro, 2009. Si-substituted hydroxyapatite nanopowders: synthesis, thermal stability and sinterability. *Materials Research Bulletin*, 44: 345-354.
- Blackwood, D. and K. Seah, 2009. Electrochemical cathodic deposition of hydroxyapatite: improvements in adhesion and crystallinity. *Materials Science and Engineering:C*, 29: 1233-1238.
- Ciobanu, C.S., S.L. Iconaru, C.L. Popa, *et al.*, 2011). Evaluation of samarium doped hydroxyapatite, ceramics for medical application: Antimicrobial Activity. *Journal of Nanomaterials*, pp: 1-11.
- Claudia, S., L. Herdocia and L.L. Simara, *et al.*, 2015. Evaluation of synthesized nanohydroxyapatite-nanocellulose composites as biocompatible scaffolds for applications in bone tissue engineering. *Journal of Nanomaterials*, pp: 1-9.
- Darimont, G., R. Cloots, E. Heinen, L. Seidel and R. Legrand, 2002. In vivo behaviour of hydroxyapatite coatings on titanium implants: A quantitative study in the rabbit. *Biomaterials*, 23: 2569-2575.
- Eriksson, M., Y. Liu, J. Hu, L. Gao, M. Nygren and Z. Shen, 2011. Transparent hydroxyapatite ceramics with nanograin structure prepared by high pressure spark plasma sintering at the minimized sintering temperature. *Journal of the European Ceramic Society*, 31: 1533-1540.
- Galindo, T.G.P., T. Kataoka and M. Tagaya, 2015. Morphosynthesis of Zn-substituted stoichiometric and carbonate hydroxyapatite nanoparticles and their cytotoxicity in fibroblasts. *Journal of Nanomaterials*, pp: 1-8.
- Hayakawa, T., M. Yoshinari, H. Kiba, H. Yamamoto, K. Nemoto and J. Jansen, 2002. Trabecular bone response to surface roughened and calcium phosphate (Ca-P) coated titanium implants. *Biomaterials*, 23: 1025-1031.
- Huang, J., Y.W. Lin, X.W. Fu, S.M. Best, R.A. Brooks, N. Rushton and W. Bonfield, 2007. Development of nano-sized hydroxyapatite reinforced composites for tissue engineering scaffolds. *Journal of Materials Science: Materials in Medicine*, 18: 2151-2157.
- John Michel, Matthew Penna & Juan Kochen, *et al.*, 2015. Recent advances in hydroxyapatite scaffolds containing mesenchymal stem cells. *Stem Cells International*, pp: 1-13.
- Kong, L.B., J. Ma and F. Boey, 2002. Nanosized hydroxyapatite powders derived from coprecipitation process, *Journal of Materials Science*, 37(6): 1131-1134.
- Laura, C.R., N.I. Avram and A.M. Georgiana *et al.*, 2015. Tetracycline loaded collagen/hydroxyapatite composite materials for biomedical applications. *Journal of Nanomaterials*, pp: 1-5.
- Liu, F.W., B. Sun, X.Z. Jiang, S.S. Aldeyab, Q.H. Zhang and M.F. Zhu, 2014. Mechanical properties of dental resin/composite containing urchin-like hydroxyapatite. *Dental Materials*, 30: 1358-1368.
- Lv, Q., L. Nair and Laurencin, 2009. C.T. Fabrication, characterization, and in vitro evaluation of poly(lactic acid glycolic acid)/nano-hydroxyapatite composite microsphere-based scaffolds for bone tissue engineering in rotating bioreactors. *Journal of Biomedical Materials Research*, 91: 679-691.
- Makela, K.T., A. Eskelinen, P. Pulkkinen, P. Paavolainen and V. Remes, 2008. Total hip arthroplasty for primary osteoarthritis in patients fifty-five years of age or older. An analysis of the Finnish arthroplasty registry. *The Journal of Bone and Joint Surgery. American Volume*, 90: 2160-2170.
- Meejoo, S., W. Maneerprakorn and P. Winotai, 2006. Phase and thermal stability of nanocrystalline hydroxyapatite prepared via microwave heating. *Thermochimica Acta*, 447: 115-120.
- Sasikumar, S and R. Vijayaraghavan, 2006. Low temperature synthesis of nanocrystalline hydroxyapatite from egg shells by combustion method. *Trends in Biomaterials and Artificial Organs*, 19: 70-3.
- Sekar, C., P. Kanchana, R. Nithyaselvi and E.K. Girija, 2009. Effect of fluorides (KF and NaF) on the growth of dicalcium phosphate dihydrate (DCPD) crystal. *Materials Chemistry and Physics*, 115: 21-27.
- Singh, A., 2012. Hydroxyapatite a biomaterial: Its chemical synthesis, characterization and study of biocompatibility prepared from shell of garden snail, *Helix aspersa*. *Bulletin of Materials Science.*, 35: 1031-8.
- Sooksaen, P., N. Pongsuwan and S. Karawatthanaworakul *et al.*, 2015. Formation of porous apatite layer during in vitro study of hydroxyapatite-aw based glass composites. *Advances in Condensed Matter Physics*, pp: 1-9.
- Trombelli, L., A. Simonelli, M. Pramstraller, U.M.E. Wikesjo and R. Farina, 2010. Single flap approach with and without guided tissue regeneration and a hydroxyapatite biomaterial in the management of intraosseous periodontal defects. *Journal of Periodontology*, 81: 1256-1263.
- Vallet-Regi, M. and J.M. Gonzalez-Calbet, 2004. Calcium phosphates as substitution of bone tissues. *Progress in Solid State Chemistry*, 32: 1-31.
- Varma, H.K, and B.S. Suresh, 2005. Synthesis of calcium phosphate bioceramics by citrate gel pyrolysis method. *Ceramics International*, 31: 109-14.
- Wang, J. and L.L. Shaw, 2009. Synthesis of high purity hydroxyapatite nanopowder via sol-gel combustion process, *Journal of Medicine*, 20(6): 1223-1227.
- Wu, X.H., Z.Y. Wu, J.C. Su, Y.G. Yan, B.Q. Yu, J. Wei and L.M. Zhao, 2015. Nano-hydroxyapatite promotes self-assembly of honeycomb pores in poly(L-lactide) films through breath-figure method and MC3T3-E1 cell functions. *RSC Advances*, 5: 6607-6616.
- Yang, Y., J.L. Ong and J. Tian, 2002. Rapid sintering of hydroxyapatite by microwave processing, *Journal of Materials Science Letters*, 21: 67-69.
- Zhang, X. and K.S. Vecchio, 2007. Hydrothermal synthesis of hydroxyapatite rods, *Journal of crystal Growth*, 308(1): 133-140.